Published in final edited form as:
J Biol Chem. 2002 August 16; 277(33): 30198–30207. doi:10.1074/jbc.M204736200.

Cooperative Binding of the Cytoplasm to Vacuole Targeting Pathway Proteins, Cvt13 and Cvt20, to Phosphatidylinositol 3-Phosphate at the Pre-autophagosomal Structure Is Required for Selective Autophagy*

Daniel C. Nice[‡], **Trey K. Sato**[§,¶], **Per E. Stromhaug**[‡], **Scott D. Emr**[§,‖], and **Daniel J. Klionsky**[‡,**]

[‡]Department of Molecular, Cellular, and Developmental Biology and the Department of Biological Chemistry, University of Michigan, Ann Arbor, Michigan 48109

[§]Department of Cellular and Molecular Medicine and Howard Hughes Medical Institute, University of California School of Medicine, San Diego, La Jolla, California 92093

Abstract

Autophagy is a catabolic membrane-trafficking mechanism involved in cell maintenance and development. Most components of autophagy also function in the cytoplasm to vacuole targeting (Cvt) pathway, a constitutive biosynthetic pathway required for the transport of aminopeptidase I (Ape1). The protein components of autophagy and the Cvt pathway include a putative complex composed of Apg1 kinase and several interacting proteins that are specific for either the Cvt pathway or autophagy. A second required complex includes a phosphatidylinositol (PtdIns) 3-kinase and associated proteins that are involved in its activation and localization. The majority of proteins required for the Cvt and autophagy pathways localize to a perivacuolar pre-autophagosomal structure. We show that the Cvt13 and Cvt20 proteins are required for transport of precursor Ape1 through the Cvt pathway. Both proteins contain phox homology domains that bind PtdIns(3)P and are necessary for membrane localization to the pre-autophagosomal structure. Functional phox homology domains are required for Cvt pathway function. Cvt13 and Cvt20 interact with each other and with an autophagy-specific protein, Apg17, that interacts with Apg1 kinase. These results provide the first functional connection between the Apg1 and PtdIns 3-kinase complexes. The data suggest a role for PtdIns(3)P in the Cvt pathway and demonstrate that this lipid is required at the pre-autophagosomal structure.

*This work was supported in part by United States Public Health Service Grants GM53396 (to D. J. K.) and CA58689 (to S. D. E.) from the National Institutes of Health. The costs of publication of this article were defrayed in part by the payment of page charges. This article must therefore be hereby marked "*advertisement*" in accordance with 18 U.S.C. Section 1734 solely to indicate this fact.

** To whom correspondence should be addressed: Dept. of Molecular, Cellular, and Developmental Biology, University of Michigan, Ann Arbor, MI 48109. Tel.: 734-615-6556; Fax: 734-647-0884; klionsky@umich.edu..
¶Present address: Dept. of Cell Biology, The Scripps Research Institute, La Jolla, CA 92037.
‖Supported as an investigator of the Howard Hughes Medical Institute.

Autophagy (Apg)[1] and the cytoplasm to vacuole targeting (Cvt) pathway are distinct membrane trafficking processes that share overlapping mechanistic components. During vegetative conditions, these components are constitutively employed in a biosynthetic capacity by the Cvt pathway. However, under nutrient starvation conditions, intracellular signaling events induce the autophagic pathway, enabling the degradative recycling of proteins and organelles in the lysosome-like vacuole of yeast (1–4). Efficient regulatory mechanisms are necessary to balance these biosynthetic and degradative activities and maintain cellular homeostasis.

The majority of *cvt* mutants is allelic with *apg* and *aut* mutants that are defective in autophagy (1,2). The characterization of their gene products has begun to delineate the molecular events of the Cvt and autophagy pathways (reviewed in Refs. 5 and 6). There is significant overlap between the targeting and transport mechanisms of these pathways; however, there also exist proteins specific for each. Interestingly, the specific components appear to interact directly or indirectly with a central component, Apg1. Apg1 is a Ser/Thr protein kinase, which is required for both the Apg and Cvt pathways (7–9). The substrate of Apg1 kinase has not been identified, although Apg1 is known to be involved in autophosphorylation (7). Apg1 catalytic activity is presumably regulated through the association of specific proteins such as Apg13, another component required for both the Cvt pathway and autophagy (8–10). Apg13 interacts with Vac8, a Cvt-specific protein initially characterized as functioning in vacuolar inheritance (9, 11). The Apg1 kinase also physically interacts with Cvt9 and Apg17, proteins that are specific for the Cvt and Apg pathways, respectively (8,12).

A second complex that is required for both the Cvt and autophagy pathways includes the yeast PtdIns 3-kinase Vps34. This lipid kinase functions as part of a core complex, consisting of Vps34, Vps15, and Vps30/Apg6. Either Vps38, which is required for Prc1 transport, or Apg14, which is required for the autophagy and Cvt pathways, are also part of the complex (13). The association of Vps38 or Apg14 appears to confer specificity, perhaps by targeting the PtdIns 3-kinase to its functional location. Both the Apg1 kinase and the Apg14-containing lipid kinase complex localize to perivacuolar punctate structures. At present, a direct connection between these complexes has not been established.

To gain a better understanding of the molecular mechanisms involved in the Cvt and autophagy pathways, we carried out a systematic analysis of a yeast ORF deletion library. Our screen for strains defective for import of precursor Ape1 (prApe1) identified several previously uncharacterized mutants. Two of these mutants, yjl036w/*snx4* and ydl113c, renamed *cvt13* and *cvt20*, respectively, correspond to genes that encode proteins reported to interact with Apg17 by the two-hybrid assay (14). In addition, both proteins contain phox homology (PX) domains. The PX domain is an ~120 amino acid domain that functions as a phosphoinositide-binding module. Protein-lipid interactions enable the PX domain specifically to target proteins to organelle membranes. Through regulation of intracellular localization, the PX domain has been implicated in a wide variety of cellular processes including cell growth, intracellular signaling, cytoskeletal organization, neutrophil defense, protein transport, and vesicular trafficking (reviewed in Refs. 15 and 16). A recent analysis extended phosphoinositide binding to all 15 PX domains encoded by the *Saccharomyces cerevisiae* genome (17). In most cases, however, a connection has not yet been made between the PX domain and physiological function.

In this paper we show that Cvt13 and Cvt20 interact with a component of the Apg1 kinase complex and are specifically required for the Cvt pathway. The PX domains within Cvt13 and

[1]The abbreviations used are: Apg, autophagy; Ape1, aminopeptidase I; CFP, cyan fluorescent protein; Cvt, cytoplasm to vacuole targeting; FM 4-64, *N*-(triethylammoniumpropyl)-4-(*p*-diethylaminophenylhexatrienyl) pyridinium dibromide; GFP, green fluorescent protein; ORF, open reading frame; prApe1, precursor Ape1; Pgk1, phosphoglycerate kinase; Pho8, alkaline phosphatase; Prc1, carboxypeptidase Y; PtdIns(3)P, phosphatidylinositol 3-phosphate; PX, phox homology; YFP, yellow fluorescent protein; PIPES, 1,4-piperazinediethanesulfonic acid; GST, glutathione *S*-transferase; HA, hemagglutinin; SNXs, sorting nexins.

Cvt20 drive PtdIns(3)P-specific recruitment to a perivacuolar structure. Mutations in the PX domain block function. Finally, we demonstrate that correct localization of Cvt13 and Cvt20 requires the synthesis of PtdIns(3)P by the Apg14-containing lipid kinase complex at the pre-autophagosomal structure.

EXPERIMENTAL PROCEDURES

Strains and Media

The *S. cerevisiae* knockout library in strains BY4742 and BY4743 was purchased from ResGen™ (Invitrogen). The strains used in this study are listed in Table I. The *cvt13*Δ, *cvt20*Δ, and *apg17*Δ strains were generated by PCR-mediated disruption of the YJL036w, YDL113c, and YLR423c loci, respectively, using amplified sequences from either the *S. cerevisiae TRP1* gene, the *Saccharomyces kluyveri HIS3* gene, or the *Escherichia coli kan*^{r} gene (18) flanked by sequences homologous to the *CVT13*, *CVT20,* or *APG17* coding sequences. All primer sequences will be made available upon request. PCR-based integration of *YFP* at the 3′ end of *CVT13* and *CVT20* was used to generate strains expressing fusion protein under control of the native *CVT13* or *CVT20* promoter. The template for integration of YFP was pDH5 (19).

Media for growth of yeast strains, starvation, and induction of peroxisomes were described previously (20).

Materials and Antiserum

The preparation of antisera to Ape1 (21), Fox3 (22), Prc1, and Pho8 (23) were described previously. Antibodies to GST and the hemagglutinin (HA) and c-Myc epitopes were from Santa Cruz Biotechnology (Santa Cruz, CA). Anti-mouse horseradish peroxidase conjugate was from Zymed Laboratories Inc. (South San Francisco, CA). Antiserum to Pgk1 and Apg13 was generously provided by Dr. Jeremy Thorner (University of California, Berkeley) and Dr. Yoshinori Ohsumi (National Institute for Basic Biology, Okazaki, Japan), respectively. Other reagents were identical to those described previously (20,24,25).

Plasmid Constructions

A carboxyl-terminal fusion of HA to Cvt13 (pCVT13-HA(426)) was made by PCR amplification of the *CVT13* ORF and upstream sequence from genomic DNA and ligation into pRS426–3xHA. Additional details of the plasmid constructions will be provided upon request. To construct a carboxyl-terminal fusion of GFP to Cvt13, GFP was excised from pRS416GFP (26) using *Eag*I and *Xho*I. After *Eag*I, but prior to *Xho*I digestion, the 5′ overhang was filled in, creating a blunt end on GFP. Plasmid pCVT13-HA was digested with *Sma*I and *Xho*I to remove the DNA encoding the HA epitope and subsequently ligated with GFP, yielding pCVT13-GFP(426).

Amino-terminal fusions of protein A to Cvt13 (pProtA-CVT13(424)), Cvt20 (pProtA-CVT20 (424)), and Apg17 (pProtA-APG17(424)) were made by PCR amplification of the corresponding ORFs and ligation into the *Cla*I/*Sal*I sites of pRS424-CuProtA (27).

The amino-terminal GFP fusion plasmids pGFP-CVT20(416), pGFP-CVT20(415) (pPS108), and pGFP-APG17(426) were made by excising *CVT20* or *APG17* from pProtA-CVT20 or pProtA-APG17 with *Cla*I and *Sal*I and inserting into the *Cla*I/*Sal*I sites of pCuGFP(416) or pCuGFP(426), respectively (25).

To construct amino-terminal HA fusion plasmids, the 3xHA epitope was PCR-amplified from pRS416–3xHA. The PCR product was digested with *Spe*I and *Cla*I. Plasmid pProtA-CVT20

was digested with *Spe*I and *Cla*I to remove the DNA encoding protein A and subsequently ligated with the above PCR product, yielding pHA-Cvt20(416,424).

DNA encoding the PX domain of Cvt20 was amplified by PCR with primers containing 5′ restriction enzyme sites that allow for in-frame gene fusions with the carboxyl terminus of GST. Amplification included the DNA encoding the PX domain of Cvt13 (amino acids 156–295) and Cvt20 (amino acids 173–301). PCR product and plasmid pGEX-KG (Amersham Biosciences) were digested with the appropriate restriction enzymes and ligated to generate plasmid pGEX-KG-CVT13PX and pGEX-KG-CVT20PX.

Plasmids pCvt13^{Y79A}-GFP(416), pCvt13^{Y79A}-HA(416), pGFP-Cvt20^{Y193A}(416), and pGFP-Cvt20^{Y193A}(415) (pPS109) were constructed using the QuikChange™ Site-directed Mutagenesis Kit (Stratagene). Plasmids pCu-APG13(426) (9), pCVT19-CFP(414), pCuCFP-CVT9(424), and pCuCFP-AUT7(424) (27) were described previously.

Pulse/Chase, Nitrogen Starvation, and Pexophagy

Pulse/chase immunoprecipitation, nitrogen starvation, and pexophagy experiments were conducted as described previously (2,22,28).

Alkaline Phosphatase Enzyme Assay

Induction of autophagy was estimated by measuring the activity of alkaline phosphatase from Pho8Δ60 with *p*-nitrophenyl phosphate as substrate essentially according to methods published previously (29). Protein concentrations were determined using the BCA protein assay (Pierce).

Subcellular Fractionation

For subcellular fractionation experiments *cvt13*Δ (D3Y108) cells transformed with the pCVT13-HA(416) plasmid or *cvt20*Δ (D3Y109) cells transformed with the pHA-CVT20(426) plasmid were grown to midlog phase in SMD and then converted to spheroplasts as described previously (30). Spheroplasts were subjected to differential lysis in PS200 lysis buffer (20 mM PIPES, pH 6.8, 200 mM sorbitol) containing 5 mM $MgCl_2$ essentially as described previously (25). Fractionated samples were subjected to immunoblot analysis.

Protein A Affinity Isolation Analyses

For isolation of protein A fusion proteins and associated proteins, 30 A_{600} equivalents of yeast cells were converted to spheroplasts as described previously (30). Spheroplasts were washed in phosphate-buffered saline, pH 7.4, 1 M sorbitol, and 1 mM phenylmethylsulfonyl fluoride. Spheroplasts were lysed on ice in phosphate-buffered saline lysis buffer, and protein A was recovered on Dynabeads® as described previously (27). Bound protein was eluted with sample buffer, resolved by SDS-PAGE, and visualized by immunoblotting.

Fluorescence Microscopy

Cells were grown to midlog phase in SMD, induced with 10 μM $CuSO_4$ where appropriate for 1–2 h, and viewed on a Nikon E-800 fluorescent microscope as described previously (27). FM 4-64 labeling was as described previously (12).

Protein Purification and Protein-Lipid Overlay Assays

GST-Cvt20 PX domain fusion protein was purified from glutathione-Sepharose beads by elution with reduced glutathione according to manufacturer's specifications. Purified protein was then desalted with PD-10 columns and concentrated to 5 μg/ml with Centriprep YM-30 centrifugal filters. Protein-lipid overlay assays were conducted as described previously (24, 31). Membranes were incubated with purified GST-Cvt13 and GST-Cvt20 PX domains at 0.05

μg/ml overnight at 4 °C. Binding of GST fusions to phosphoinositides was detected by enhanced chemiluminescence. No binding of GST alone to phosphoinositides was detected.

RESULTS

cvt13Δ and cvt20Δ Cells Are Specifically Defective in the Cvt Pathway

In order to develop a comprehensive understanding of the protein components involved in cytoplasm to vacuole protein transport pathways, we undertook a systematic analysis of the yeast ORF deletion library. Each strain was initially screened for the accumulation of precursor aminopeptidase I (prApe1). The vacuolar hydrolase, aminopeptidase I (Ape1), is synthesized in the cytosol as a precursor protein and is transported to the vacuole through the Cvt or Apg pathway (reviewed in Refs. 5 and 6).

Two of the mutants that we identified were *cvt13* (YJL036w/*snx4*) and *cvt20* (YDL113c). Both mutants accumulated the precursor form of Ape1 in rich medium, indicating a block in the Cvt pathway (Fig. 1*A*). The *cvt13* mutant was initially isolated in a random screen for mutants defective in prApe1 maturation (1), but the corresponding gene had not been identified. A yeast genome database search for sequences with similarity to human sorting nexins (SNXs) identified a number of genes, including the open reading frame *YJL036w* (32). The sequence similarity of YJL036w with human *SNX4* grouped it as the yeast ortholog SceSNX4. However, due to its functional placement within the Cvt transport pathway, *YJL036w* was renamed *CVT13*. Sequencing of the *YJL036w* gene from the *cvt13* mutant revealed that deletion of the guanine base at position 113 of the ORF changed amino acid 38 and induced a frameshift.[2] No function for the *CVT20* gene product has been shown previously in prApe1 transport.

To determine whether these proteins functioned in additional vacuolar transport pathways, we examined the processing of resident vacuolar hydrolases carboxypeptidase Y (Prc1) and alkaline phosphatase (Pho8). Prc1 and Pho8 transit to the vacuole through the CPY and ALP pathways, respectively, and are useful marker proteins to monitor the state of these transport processes (33). Both Prc1 and Pho8 undergo glycosylation in the endoplasmic reticulum and Golgi complex and are proteolytically processed in the vacuole. The molecular mass shifts that correspond to these modifications provide a convenient means to monitor the transport process. Yeast cells were subjected to a radioactive pulse/chase analysis to determine the kinetics of protein delivery to the vacuole. Wild type, *cvt13*Δ, and *cvt20*Δ cells efficiently processed both proteins, although the *cvt13*Δ strain displayed a weak defect in processing of Prc1 and accumulated ~5% of the protein in the p2 Golgi-modified form (Fig. 1*A*). These results suggest that the Cvt13 and Cvt20 proteins do not have major functions in Prc1 and Pho8 vacuolar delivery pathways.

Precursor Ape1 is transported to the vacuole through both the Cvt pathway and autophagy (2). Most of the characterized *apg*/*cvt* mutants are defective in delivery through both pathways and accumulate prApe1 under both rich and starvation conditions (reviewed in Ref. 34). Some mutants, however, are specific to each pathway. For example, *cvt9*Δ and *vac8*Δ strains are blocked in the Cvt pathway but are not completely blocked for autophagic import. These mutants are able to “reverse” their prApe1 accumulation defect through starvation-induced autophagy (9,12). In wild type cells, prApe1 is matured with a half-time of ~30 min in synthetic minimal medium containing nitrogen (SMD). In contrast, very little mature Ape1 was detected in *cvt13*Δ and *cvt20*Δ cells under these conditions (Fig. 1*B*). The *cvt13* and *cvt20* mutants reversed the accumulation defect and processed prApe1 when shifted to SD-N, nitrogen starvation conditions (Fig. 1*B*). As a control, we examined the *apg1*Δ mutant. Apg1 is a Ser/

[2]Z. Xie and H. Abeliovich, unpublished results.

Thr kinase essential for both Cvt transport and autophagy (7–9). As expected, *apg1*Δ cells did not import prApe1 under either condition.

High throughput two-hybrid analysis indicated a possible three-way interaction between Cvt13, Cvt20, and Apg17 (8,14). In contrast to *cvt9*Δ and *vac8*Δ strains, the *apg17*Δ mutant is not defective for prApe1 import through the Cvt pathway but is defective for autophagy (8,9,12). We found that *apg17*Δ cells processed prApe1, albeit with a slightly lower efficiency (Fig. 1*B*). It is thought that starvation conditions result in a signal transduction event that induces autophagy and causes the Apg/Cvt machinery to switch from the production of Cvt vesicles to the formation of autophagosomes. As a result, precursor Ape1 is selectively transported to the vacuole by autophagosomes under starvation conditions (3). Even though autophagy is defective in the *apg17*Δ mutant (8), we found that prApe1 processing occurred under starvation conditions in *apg17*Δ cells (Fig. 1*B*). This result suggests either that transport through the Cvt pathway normally continues even when the autophagic pathway is induced or that Apg17 is necessary for the negative regulation of the Cvt pathway.

The data for the *apg17*Δ strain indicate that the ability to process prApe1 under starvation conditions is not a valid measure of autophagic function. Accordingly, we utilized an alternative approach to assess further the autophagic capacity of the *cvt13*Δ and *cvt20*Δ mutant strains. Pho8Δ60 is a soluble derivative of the integral membrane vacuolar protein Pho8 (alkaline phosphatase) that lacks the transmembrane domain. Pho8Δ60 is only delivered to the vacuole through the autophagy pathway (35). Upon vacuole delivery it is matured into its active form. Cells from wild type (TN124) and the *cvt13*Δ, *cvt20*Δ, and *apg17*Δ mutant strains expressing the Pho8Δ60 protein were measured for alkaline phosphatase activity following a shift to starvation conditions. Comparable with wild type cells, alkaline phosphatase enzymatic activity in *cvt13*Δ and *cvt20*Δ cells increased significantly after shifting to SD-N (Fig. 1*C*), indicating that Pho8Δ60 delivery and subsequent processing to its enzymatically active form occurred in the vacuole. By contrast, no increase in enzyme activity was detected upon shift to SD-N in the autophagy mutant *apg17*Δ, in agreement with previous studies (8). We also examined a *cvt13*Δ *cvt20*Δ double mutant strain to determine whether the autophagic capacity of the *cvt13*Δ and *cvt20*Δ strains was due to functional overlap between these two proteins. Alkaline phosphatase enzymatic activity in the double mutant strain was comparable with wild type (data not shown), suggesting that Cvt13 and Cvt20 are not essential for autophagy. Yeast mutants defective for autophagy are unable to recycle cytosolic material and thus die rapidly upon shifting to starvation conditions. When *cvt13*Δ and *cvt20*Δ cells were shifted to SD-N, their viability was comparable with wild type cells (data not shown), further indicating that autophagy is not defective in these strains.

Peroxisomes are induced under specific nutritional conditions such as growth in oleic acid as the sole carbon source. When cells grown on oleic acid are shifted to glucose-containing medium, peroxisomes are specifically degraded by a process termed pexophagy. The molecular machinery involved in pexophagy has been shown to overlap with that of the autophagy and Cvt pathways (reviewed in Ref. 34). We examined the degradation of the peroxisomal enzyme Fox3 (thiolase) to determine the requirement of Cvt13 and Cvt20 for the specific uptake of peroxisomes by pexophagy. Cells were grown in an oleic acid-containing medium to induce peroxisomes, switched to SD-N, and the level of Fox3 monitored by immunoblotting (22). In wild type cells, Fox3 was rapidly degraded. However, Fox3 was stable in *cvt13*Δ and *cvt20*Δ cells, indicating they are defective in the uptake of peroxisomes by pexophagy (Fig. 1*D*). We did detect a very slight decrease in Fox3 over the time course examined in the *cvt13*Δ and *cvt20*Δ strains, but the level was clearly stabilized relative to the wild type strain. With the exception of Cvt19, all *cvt* and *apg* mutants characterized thus far display defects in degradation of peroxisomes by pexophagy (9,22).

Both Cvt13 and Cvt20 Distribute between the Cytosol and Punctate Structures near the Vacuole

To gain insight into the function of Cvt13 and Cvt20, we examined the localization of these proteins *in vivo* through the use of GFP fusion proteins. Expression of Cvt13-GFP under the endogenous *CVT13* promoter fully complemented the prApe1 transport defect in a *cvt13*Δ mutant, indicating that it was a functional chimera (data not shown). GFP-Cvt20 and GFP-Apg17, both under control of the *CUP1* promoter, were induced with a relatively low concentration of $CuSO_4$ (10 μ_M) for 1–2 h. GFP-Cvt20 expression fully complemented the prApe1 defect in a *cvt20*Δ mutant (data not shown). After labeling the vacuoles with the dye FM 4-64, cells expressing the various GFP constructs were examined by fluorescence microscopy. Cvt13-GFP and GFP-Cvt20 displayed both a diffuse cytosolic distribution and punctate structures near or on the surface of FM 4-64-labeled vacuoles (Fig. 2). Additional faint perivacuolar and vacuolar rim staining was also detectable. GFP-Apg17 displayed punctate structures similar to those seen with Cvt13-GFP and GFP-Cvt20, but no cytosolic staining was evident. GFP-Apg17 punctate structures were found adjacent to the vacuole, however, in contrast to Cvt13-GFP and GFP-Cvt20, they were also seen in other areas of the cell (Fig. 2).

The perivacuolar staining seen with both GFP-Cvt20 and Cvt13-GFP is reminiscent of the staining pattern seen with many of the proteins that are involved in the Apg and Cvt pathways (12,20,25,27). Although the nature of this perivacuolar structure is still unknown, it appears to play a physiological role in Cvt vesicle and autophagosome formation (27,36). We co-localized Cvt13 and Cvt20 with Cvt9, Cvt19, and Aut7 to determine whether these components localize to the same perivacuolar structure. Cvt19 is a cargo receptor or adaptor required for transport of the prApe1 complex (37), and Aut7 plays a role in vesicle formation and size regulation (25,38–40). Co-localization of Aut7, Cvt19, and Cvt9 has been demonstrated recently (27). Chromosomally expressed Cvt13-YFP or Cvt20-YFP displayed punctate structures that co-localized with Cvt19-CFP, CFP-Cvt9, and CFP-Aut7 (Fig. 3*A*). A number of cells expressing Cvt13-YFP and Cvt20-YFP also displayed diffuse cytosolic staining. These results indicate that a population of Cvt13 and Cvt20 localizes to the same perivacuolar structure as Cvt9, Cvt19, and Aut7.

The localization of some Apg/Cvt proteins has been shown to depend on other proteins within these pathways. For example, membrane recruitment of Aut7 requires the function of the Apg12-Apg5 and the Aut1 conjugation systems (25,40). We examined the localization of Cvt19-CFP and its co-localization with YFP-Cvt9 and YFP-Aut7 in the *cvt13*Δ and *cvt20*Δ strains. Tagged proteins were co-expressed in all combinations, and the localization of each protein appeared normal (Fig. 3*B* and data not shown). These data suggest that Cvt19, Cvt9, and Aut7 localize to the perivacuolar structure independent of Cvt13 and Cvt20. Furthermore, these results imply that Cvt13 and Cvt20 are not required for the functions associated with these proteins, such as Cvt19-prApe1 complex binding (37), and Aut7-dependent membrane expansion (38).

Cvt13 and Cvt20 Fractionate with Membranes

To extend the localization analysis *in vitro*, we examined the subcellular localization of Cvt13 and Cvt20 by differential centrifugation. The *cvt13*Δ and *cvt20*Δ strains were transformed with plasmids pCVT13-HA and pHA-CVT20, respectively, and grown to midlog phase in SMD. The expression of the respective HA epitope-tagged proteins completely complemented the prApe1 accumulation defect in the *cvt13*Δ and *cvt20*Δ strains (data not shown), indicating that the addition of the HA epitope did not alter Cvt13 and Cvt20 function. Spheroplasts were lysed and centrifuged to separate the lysates into low speed supernatant (S13) and pellet (P13) fractions (see “Experimental Procedures”). The S13 fraction was then further separated into

high speed supernatant (S100) and pellet (P100) fractions. Immunoblot analysis revealed that HA-tagged Cvt13 and Cvt20 were distributed essentially equally throughout all pellet and supernatant fractions (data not shown), suggesting the presence of both cytosolic and membrane-associated protein. The distribution of the cytosolic protein, phosphoglycerate kinase (Pgk1), confirmed separation of membrane and soluble proteins.

The nature of the Cvt13 and Cvt20 pellet association was examined by treating the pellet fraction with various reagents. Treating the pellet fractions with 1 M salt, 3 M urea, or 1% Triton X-100 resulted in partial stripping of HA-tagged Cvt13 and Cvt20 into the supernatant fraction. However, both proteins were completely removed from the pellet fraction by extraction with 0.1 M Na_2CO_3, pH 10.5 (data not shown). These results indicate that Cvt13 and Cvt20 exist as both cytosolic and peripheral membrane proteins, and are in agreement with the *in vivo* fluorescent analysis that revealed both a punctate and diffuse cytosolic pool of both proteins (Fig. 2).

Cvt13, Cvt20, and Apg17 Interact

The analyses of GFP localization patterns along with two-hybrid studies suggested that Cvt13, Cvt20, and Apg17 may compose a protein complex (14). Previously published data have demonstrated that Apg1 physically interacts with Apg17, an autophagy-specific component, and Cvt9, a Cvt-specific component (8,12). To investigate potential physical associations among Cvt13, Cvt20, and Apg17, a series of affinity purification experiments was undertaken with fusions to protein A. Either protein A alone or a protein A fusion was co-expressed in combination with Cvt13-HA. The expression of protein A-tagged Cvt13 or Cvt20 complemented the prApe1 accumulation defect in *cvt13*Δ and *cvt20*Δ strains, respectively (data not shown). Cells were grown to midlog phase, converted to spheroplasts, and lysed in the presence of detergent. Protein A and associated proteins were then affinity-isolated by binding to IgG-coupled Dynabeads as described under “Experimental Procedures.” The recovered proteins were separated by SDS-PAGE and examined by immunoblot. Cvt13-HA bound to protein A-Cvt13, protein A-Cvt20, and protein A-Apg17 (Fig. 4). Cvt13-HA did not bind to protein A alone, indicating that the interaction with Cvt13-HA was dependent on Cvt13, Cvt20, or Apg17 fused to protein A. These data support the existence of a protein complex with a three-way physical interaction between Cvt13, Cvt20, and Apg17. This complex may also include multiple copies of Cvt13.

At least two proteins that interact with Apg1 modulate its kinase activity. One of these proteins, Apg13, is hyperphosphorylated in a Tor-dependent manner under rich media conditions. This form of Apg13 has a low affinity for Apg1, and under these conditions *in vitro* Apg1 kinase activity is reduced (8). Starvation results in dephosphorylation of Apg13, a greater affinity for Apg1, and an increase in Apg1 kinase activity *in vitro*. It is possible that the phosphorylation state of Apg13 is the signal that regulates the conversion between the Cvt and Apg pathways. We determined whether the phosphorylation state of Apg13 was altered in the *cvt13*Δ, *cvt20*Δ, or *apg17*Δ mutants. Wild type or mutant cells were grown in SMD and shifted to starvation conditions for 10 min, and Apg13 was examined by immunoblot (Fig. 5). In both wild type and mutant cells, Apg13 was seen primarily as the hyperphosphorylated form in SMD prior to shifting to starvation conditions. A smaller population of the protein was also detected as the hypophosphorylated form. Within 10 min in SD-N medium, the protein was efficiently dephosphorylated and migrated at a single position on the gel in all of the strains examined. Shifting the culture back to SMD resulted in rapid hyperphosphorylation (data not shown). These results suggest that Cvt13, Cvt20, and Apg17 do not affect the Cvt and Apg pathways by regulating the phosphorylation of Apg13.

The PX Domains of Cvt13 and Cvt20 Bind the Phosphoinositide PtdIns(3)P and Are Necessary for Cvt Transport

The PX domain has been identified as a novel ~120-residue domain that functions as a phosphoinositide-binding module (24). Sequence database analyses identified a number of proteins in yeast, including Cvt13 and Cvt20, that contain a PX domain (17). However, the *in vivo* role of the PX domain for Cvt13 and Cvt20 has not been addressed. The PX domain binding specificity of Cvt13 and Cvt20 was examined using a protein-lipid binding assay (31). Nitrocellulose membranes were spotted with decreasing amounts of various phosphoinositides and incubated with affinity-purified PX domains of Cvt13 or Cvt20 fused to glutathione *S*-transferase (GST) (Fig. 6, *A* and *B*). Both GST-PX domain fusions displayed a preferential interaction with PtdIns(3)P and a weaker interaction with PtdIns(3,5)P_2.

The *VPS34* gene encodes the sole yeast PtdIns 3-kinase (41). Fab1 is a PtdIns(3)P 5-kinase, which phosphorylates PtdIns(3)P to produce PtdIns(3,5)P_2 (42). Localization of Cvt13-GFP and GFP-Cvt20 was examined in both *vps34*Δ and *fab1*Δ strains to confirm the PtdIns(3)P specificity and determine whether membrane binding was dependent upon phosphoinositide synthesis. Cvt13-GFP and GFP-Cvt20 punctate staining completely redistributed into the cytosol in the *vps34*Δ strain (Fig. 6*C*). In contrast, fluorescence staining in the *fab1*Δ strain remained similar to that seen in wild type cells, with distribution between the cytosol and punctate structures. These data indicate that PtdIns(3)P binding is necessary for Cvt13 and Cvt20 membrane localization to perivacuolar punctate structures.

Analysis of the PX domain by NMR spectroscopy identified a basic binding pocket and membrane attachment loop as the structural basis for PtdIns(3)P binding (24). Altering a key tyrosine residue in one of two basic motifs, RR(Y/F) (where R is arginine, Y is tyrosine, and F is phenylalanine) within the binding pocket (Fig. 7*A*), has been shown to block phosphoinositide-binding (24,43). A Tyr to Ala mutation of the highly conserved RRY motif was generated within the PX domain of Cvt13 and Cvt20. Cvt13^{Y79A}-GFP and GFP-Cvt20^{Y193A} punctate staining completely redistributed to the cytosol (Fig. 7*B*). Immunoblot analysis indicated that Cvt13^{Y79A}-GFP and GFP-Cvt20^{Y193A} were stable and corresponded to predicted molecular weights (data not shown). Thus, depleting the cell of PtdIns(3)P or mutating the PX domain abolished intracellular punctate localization of Cvt13 and Cvt20.

Next, we investigated the role of Cvt13 and Cvt20 PX domains in Cvt transport. Expression of Cvt13^{Y79A}-GFP in the *cvt13*Δ strain showed an incomplete block in prApe1 processing (data not shown). A similar result was seen with GFP-Cvt20^{Y193A} expressed in the *cvt20*Δ background. Because Cvt13 and Cvt20 physically interact, partial complementation of prApe1 transport in these single PX domain mutants may have occurred through membrane targeting by the wild type PX domain partner. To address this possibility, we generated a *cvt13*Δ *cvt20*Δ double mutant strain expressing Cvt13-HA, Cvt13^{Y79A}-HA, GFP-Cvt20, and GFP-Cvt20^{Y193A} in varying combinations. When the PX domain of either Cvt13 or Cvt20 contained the Tyr to Ala mutation, prApe1 processing was reduced to ~50%. However, when both PX domains contained the Tyr to Ala mutation, prApe1 processing was almost completely blocked (Fig. 7*C*). Thus, Cvt13 and Cvt20 PtdIns(3)P-binding capacity is necessary for Cvt transport.

Apg14, a Component of the PtdIns 3-Kinase Complex, Is Necessary for Cvt13 and Cvt20 Punctate, Perivacuolar Localization

To investigate further possible Cvt13 and Cvt20 connections with the PtdIns 3-kinase complex, co-localization with Cvt19 was examined in the *apg14*Δ mutant strain. Apg14 is a component of the PtdIns 3-kinase complex required for the Cvt pathway and autophagy but not for the CPY pathway. As shown in Fig. 3, Cvt13-YFP and Cvt20-YFP co-localize with Cvt19-CFP in wild type cells. Similarly, Cvt19-CFP co-localization with Cvt13-YFP and Cvt20-YFP was

normal in *aut7*Δ cells that are defective in the Cvt pathway and autophagy (Fig. 8). In contrast, punctate structures labeled with Cvt13-YFP or Cvt20-YFP were less frequent and of lower intensity in the *apg14*Δ strain (Fig. 8). Furthermore, in those cells that displayed punctate staining for Cvt13-YFP or Cvt20-YFP, the labeled structures seldom co-localized with Cvt19-CFP (Fig. 8). Loss of Cvt13 and Cvt20 punctate perivacuolar localization in this mutant strain occurred concomitant with an increased staining of more diffuse punctate structures near the vacuole and in the cytosol. These results suggest Apg14 may be dispensable for Cvt13 and Cvt20 PtdIns(3)P binding at other membranes that contain this lipid, such as the endosome, but necessary for recruitment to the pre-autophagosomal structure where they participate in Cvt transport. This result is in contrast to the complete loss of punctate staining seen with the *vps34*Δ strain that completely lacks PtdIns 3-kinase activity (Fig. 6). These data represent the first evidence of the requirement of PtdIns(3)P at the presumed site of pre-autophagosome/Cvt vesicle formation.

DISCUSSION

Cvt13 and Cvt20 Are PX Domain Proteins That Associate with Components of the Apg1 Kinase Signaling Complex

The studies presented in this paper have defined two new proteins in the Cvt pathway, Cvt13 and Cvt20. These proteins contain PX domains that bind to PtdIns(3)P. Both Cvt13 and Cvt20 are localized to a punctate perivacuolar structure, and binding to PtdIns(3)P is critical for this localization. Finally, correct localization of both proteins is necessary for import of prApe1 through the Cvt pathway. Cvt13 is the first Cvt pathway-specific protein that has been characterized that has a mammalian homolog, Snx4 (32). This is an interesting finding because there are no data at present demonstrating that the Cvt pathway exists in any organism other than *S. cerevisiae*.

Autophagy and the Cvt pathway are distinct membrane trafficking processes that share overlapping mechanistic components. These components include the Apg1 kinase and its associated proteins, Apg13, Apg17, and Cvt9 (8,12). A second set of proteins required for both pathways is the PtdIns 3-kinase complex composed of Vps34, Vps15, Apg6, and Apg14 (13). A separate PtdIns 3-kinase complex containing Vps38 instead of Apg14 is needed for protein transport through the CPY pathway. This latter complex is responsible for the synthesis of the majority of PtdIns(3)P in the cell and at present it has not been possible to assess directly the site of action of the Apg14-dependent PtdIns 3-kinase.

Cvt13 and Cvt20 were shown to interact with Apg17 by a two-hybrid screen (14). These proteins were also identified as belonging to a family containing the PX domain (17). However, neither of these analyses provided information on the physiological roles of Cvt13 or Cvt20. We identified the *cvt13*Δ and *cvt20*Δ strains in a screen of the *S. cerevisiae* deletion library as being defective in the processing of the vacuolar hydrolase Ape1. Both proteins are necessary for vacuole delivery of prApe1, and the mutant strains accumulated the precursor form of Ape1 in rich medium, indicating a defect in the Cvt pathway (Fig. 1). In contrast, the *cvt13*Δ and *cvt20*Δ strains were not defective in autophagy. Other vacuolar transport systems including the CPY and ALP pathways are essentially normal in *cvt13*Δ and *cvt20*Δ cells. However, both mutants are defective in the uptake of peroxisomes by pexophagy.

Consistent with two-hybrid results (14), immunoisolation experiments demonstrate that Cvt13, Cvt20, and Apg17 directly interact with each other (Fig. 4). In addition, Cvt13 forms homodimers or higher order oligomers. These data support a model in which Cvt20, Apg17, and one or more Cvt13 subunits form a protein complex. This complex may include additional components, such as Apg1, Apg13, and Vac8. Apg1 has recently been ascribed a central role in the events signaling a switch between the Cvt and autophagy pathways (8). We were unable

to detect an interaction between Apg1 and either Cvt13 or Cvt20 in our affinity isolation experiments (Fig. 4). This may simply mean that Apg1 does not interact directly with either protein, and our experimental conditions did not preserve ternary or higher order complexes. Alternatively, this result may indicate the presence of multiple complexes containing discrete subsets of proteins.

Cvt13, Cvt20, Cvt9, Cvt19, and Aut7 Co-Localize on a Punctate, Perivacuolar Structure

Biochemical analyses indicate that Cvt13 and Cvt20 are membrane-associating proteins present in both a soluble and membrane fraction. *In vivo* analyses of GFP-tagged proteins suggest that Cvt13 and Cvt20 distribute between the cytosol and punctate structures near the vacuole (Fig. 2). Recent studies have placed Apg1 and Cvt9 at a perivacuolar compartment (12,27). Various other components involved in the Cvt and Apg pathways including the autophagy/Cvt-specific PtdIns 3-kinase complex have also been localized to this pre-autophagosomal structure (27,36). Fluorescence microscopy showed Cvt13 and Cvt20 co-localization with Cvt9, Cvt19, and Aut7 (Fig. 3*A*). This perivacuolar compartment may mark the site of vesicle nucleation and cargo sequestration and has been termed the pre-autophagosomal structure (36).

Cvt13 and Cvt20 PX Domains Are PtdIns(3)P-specific Binding Modules That Direct Recruitment to a Perivacuolar Structure and Are Necessary for Cvt Transport

PX domains are involved in the targeting of various proteins to membranes that contain PtdIns (3)P. Proteins with PX domains have been implicated in a range of cellular processes (reviewed in Ref. 15). Until now, PX domain-containing proteins have not been implicated in the Cvt pathway or autophagy. A mutation in the RR(Y/F) basic motif demonstrates that Cvt13 and Cvt20 membrane association requires a functional PX domain (Fig. 7). The presence of a PX domain in both associating proteins, Cvt13 and Cvt20, may allow for increased affinity and PtdIns(3)P-binding capacity. Similarly, the selective targeting of Cvt13 and Cvt20 to perivacuolar structures may be directed through interaction with additional proteins. The PX domains in Cvt13 and Cvt20 bind PtdIns(3)P with relatively low affinity (Fig. 6;17) so that they likely require interaction with other components to direct membrane binding and membrane specificity. We are currently investigating the interaction of Cvt13 and Cvt20 with other Apg and Cvt proteins. Vps34, the yeast PtdIns 3-kinase, interacts with Vps15, a membrane-associated Ser/Thr kinase that regulates Vps34 activity (44). Vps15 and Vps34 are subunits of a core PtdIns 3-kinase complex that may function at different membrane sites, regulating different protein trafficking events (13). Vps15/Vps34 complexed with accessory proteins Vps30 and Vps38 may concentrate primarily at the Golgi, functioning in Prc1 targeting to the endosome/prevacuolar compartment. Vps15/Vps34 complexed with accessory proteins Vps30 and Apg14 may concentrate primarily at the pre-autophagosomal structure, functioning in Cvt and autophagy membrane traffic to the vacuole. Processing of prApe1 is completely blocked in *vps15*, *vps30*, *vps34*, and *apg14*, but not *vps38* mutant strains (13). Alkaline phosphatase activity assays employing Pho8Δ60 indicate severely impaired autophagic capacity in *vps15*, *vps30*, *vps34*, and *apg14* mutant cells in response to starvation. Thus, a functional autophagy/Cvt-specific PtdIns 3-kinase complex and PtdIns(3)P production is necessary for autophagy and Cvt transport, although the site of action of the Apg14-dependent PtdIns 3-kinase has not been demonstrated. PtdIns(3)P concentration by specific PtdIns 3-kinase complexes may target PX domain proteins to their site of function on discrete membrane domains. Indeed, Cvt13 and Cvt20 punctate perivacuolar localization was lost in *apg14*Δ cells (Fig. 8), suggesting that the Apg14-dependent PtdIns 3-kinase must function at the pre-autophagosomal structure.

Cvt13 and Cvt20 PtdIns(3)P binding and targeted membrane association is required for prApe1 transport through the Cvt pathway. Mutating tyrosine in the PX domain RR(Y/F) basic motif

of either Cvt13 or Cvt20 resulted in diminished prApe1 processing (Fig. 7). With only one functional PX domain, the interaction of Cvt13 and Cvt20 may enable partial, reduced capacity Cvt transport. The PX domain mutation appears to abolish localization of the protein to the punctate perivacuolar structure; however, the partial function suggests that a low level of the protein may still be binding membrane. If so, this level is below detection. Alternatively, Cvt13 and Cvt20 retain sufficient activity in the absence of efficient membrane binding of either individual protein to permit partial import of prApe1. When the PX domain of both Cvt13 and Cvt20 are mutated, Cvt transport is blocked (Fig. 7). These data indicate a direct physiological function for the yeast PX domain. Furthermore, we know that a PtdIns 3-kinase complex is required for the autophagy/Cvt pathways (13). The PX domains of Cvt13 and Cvt20 function as PtdIns(3)P-binding modules; thus these data provide the first molecular connection between the autophagy/Cvt pathways and the autophagy/Cvt specific-PtdIns 3-kinase complex.

Acknowledgments

We thank Wei-Pang Huang and Dr. John Kim for valuable discussions.

REFERENCES

1. Harding TM, Hefner-Gravink A, Thumm M, Klionsky DJ. J. Biol. Chem 1996;271:17621–17624. [PubMed: 8663607]
2. Scott SV, Hefner-Gravink A, Morano KA, Noda T, Ohsumi Y, Klionsky DJ. Proc. Natl. Acad. Sci. U. S. A 1996;93:12304–12308. [PubMed: 8901576]
3. Baba M, Osumi M, Scott SV, Klionsky DJ, Ohsumi Y. J. Cell Biol 1997;139:1687–1695. [PubMed: 9412464]
4. Scott SV, Baba M, Ohsumi Y, Klionsky DJ. J. Cell Biol 1997;138:37–44. [PubMed: 9214379]
5. Stromhaug PE, Klionsky DJ. Traffic 2001;2:524–531. [PubMed: 11489210]
6. Reggiori F, Klionsky DJ. Euk. Cell 2002;1:11–21.
7. Matsuura A, Tsukada M, Wada Y, Ohsumi Y. *Gene* (*Amst*.) 1997;192:245–250. [PubMed: 9224897]
8. Kamada Y, Funakoshi T, Shintani T, Nagano K, Ohsumi M, Ohsumi Y. J. Cell Biol 2000;150:1507–1513. [PubMed: 10995454]
9. Scott SV, Nice DC III, Nau JJ, Weisman LS, Kamada Y, Keizer-Gunnink I, Funakoshi T, Veenhuis M, Ohsumi Y, Klionsky DJ. J. Biol. Chem 2000;275:25840–25849. [PubMed: 10837477]
10. Funakoshi T, Matsuura A, Noda T, Ohsumi Y. *Gene* (*Amst*.) 1997;192:207–213. [PubMed: 9224892]
11. Wang YX, Zhao H, Harding TM, Gomes de Mesquita DS, Woldringh CL, Klionsky DJ, Munn AL, Weisman LS. Mol. Biol. Cell 1996;7:1375–1389. [PubMed: 8885233]
12. Kim J, Kamada Y, Stromhaug PE, Guan J, Hefner-Gravink A, Baba M, Scott SV, Ohsumi Y, Dunn WA Jr. Klionsky DJ. J. Cell Biol 2001;153:381–396. [PubMed: 11309418]
13. Kihara A, Noda T, Ishihara N, Ohsumi Y. J. Cell Biol 2001;152:519–530. [PubMed: 11157979]
14. Uetz P, Giot L, Cagney G, Mansfield TA, Judson RS, Knight JR, Lockshon D, Narayan V, Srinivasan M, Pochart P, Qureshi-Emili A, Li Y, Godwin B, Conover D, Kalbfleisch T, Vijayadamodar G, Yang M, Johnston M, Fields S, Rothberg JM. Nature 2000;403:623–627. [PubMed: 10688190]
15. Sato TK, Overduin M, Emr SD. Science 2001;294:1881–1885. [PubMed: 11729306]
16. Wishart MJ, Taylor GS, Dixon JE. Cell 2001;105:817–820. [PubMed: 11439176]
17. Yu JW, Lemmon MA. J. Biol. Chem 2001;276:44179–44184. [PubMed: 11557775]
18. Longtine MS, McKenzie A III, Demarini DJ, Shah NG, Wach A, Brachat A, Philippsen P, Pringle JR. Yeast 1998;14:953–961. [PubMed: 9717241]
19. Drees BL, Sundin B, Brazeau E, Caviston JP, Chen GC, Guo W, Kozminski KG, Lau MW, Moskow JJ, Tong A, Schenkman LR, McKenzie A III, Brennwald P, Longtine M, Bi E, Chan C, Novick P, Boone C, Pringle JR, Davis TN, Fields S, Drubin DG. J. Cell Biol 2001;154:549–571. [PubMed: 11489916]
20. Wang C-W, Kim J, Huang W-P, Abeliovich H, Stromhaug PE, Dunn WA Jr. Klionsky DJ. J. Biol. Chem 2001;276:30442–30451. [PubMed: 11382760]

21. Klionsky DJ, Cueva R, Yaver DS. J. Cell Biol 1992;119:287–299. [PubMed: 1400574]
22. Hutchins MU, Veenhuis M, Klionsky DJ. J. Cell Sci 1999;112:4079–4087. [PubMed: 10547367]
23. Klionsky DJ, Emr SD. EMBO J 1989;8:2241–2250. [PubMed: 2676517]
24. Cheever ML, Sato TK, de Beer T, Kutateladze TG, Emr SD, Overduin M. Nat. Cell Biol 2001;3:613–618. [PubMed: 11433291]
25. Kim J, Huang W-P, Klionsky DJ. J. Cell Biol 2001;152:51–64. [PubMed: 11149920]
26. Kim J, Dalton VM, Eggerton KP, Scott SV, Klionsky DJ. Mol. Biol. Cell 1999;10:1337–1351. [PubMed: 10233148]
27. Kim J, Huang W-P, Stromhaug PE, Klionsky DJ. J. Biol. Chem 2002;277:763–773. [PubMed: 11675395]
28. Sato TK, Darsow T, Emr SD. Mol. Cell. Biol 1998;18:5308–5319. [PubMed: 9710615]
29. Mitchell JK, Fonzi WA, Wilkerson J, Opheim DJ. Biochim. Biophys. Acta 1981;657:482–494. [PubMed: 7011403]
30. Scott SV, Klionsky DJ. J. Cell Biol 1995;131:1727–1735. [PubMed: 8557740]
31. Dowler S, Currie RA, Downes CP, Alessi DR. Biochem. J 1999;342:7–12. [PubMed: 10432293]
32. Haft CR, de la Luz Sierra M, Barr VA, Haft DH, Taylor SI. Mol. Cell. Biol 1998;18:7278–7287. [PubMed: 9819414]
33. Kim J, Scott SV, Klionsky DJ. Int. Rev. Cytol 2000;198:153–201. [PubMed: 10804463]
34. Kim J, Klionsky DJ. Annu. Rev. Biochem 2000;69:303–342. [PubMed: 10966461]
35. Noda T, Matsuura A, Wada Y, Ohsumi Y. Biochem. Biophys. Res. Commun 1995;210:126–132. [PubMed: 7741731]
36. Suzuki K, Kirisako T, Kamada Y, Mizushima N, Noda T, Ohsumi Y. EMBO J 2001;20:5971–5981. [PubMed: 11689437]
37. Scott SV, Guan J, Hutchins MU, Kim J, Klionsky DJ. Mol. Cell 2001;7:1131–1141. [PubMed: 11430817]
38. Abeliovich H, Dunn WA Jr. Kim J, Klionsky DJ. J. Cell Biol 2000;151:1025–1034. [PubMed: 11086004]
39. Ichimura Y, Kirisako T, Takao T, Satomi Y, Shimonishi Y, Ishihara N, Mizushima N, Tanida I, Kominami E, Ohsumi M, Noda T, Ohsumi Y. Nature 2000;408:488–492. [PubMed: 11100732]
40. Kirisako T, Ichimura Y, Okada H, Kabeya Y, Mizushima N, Yoshimori T, Ohsumi M, Takao T, Noda T, Ohsumi Y. J. Cell Biol 2000;151:263–276. [PubMed: 11038174]
41. Schu PV, Takegawa K, Fry MJ, Stack JH, Waterfield MD, Emr SD. Science 1993;260:88–91. [PubMed: 8385367]
42. Gary JD, Wurmser AE, Bonangelino CJ, Weisman LS, Emr SD. J. Cell Biol 1998;143:65–79. [PubMed: 9763421]
43. Kanai F, Liu H, Field SJ, Akbary H, Matsuo T, Brown GE, Cantley LC, Yaffe MB. Nat. Cell Biol 2001;3:675–678. [PubMed: 11433300]
44. Stack JH, Herman PK, Schu PV, Emr SD. EMBO J 1993;12:2195–2204. [PubMed: 8387919]
45. Robinson JS, Klionsky DJ, Banta LM, Emr SD. Mol. Cell. Biol 1988;8:4936–4948. [PubMed: 3062374]

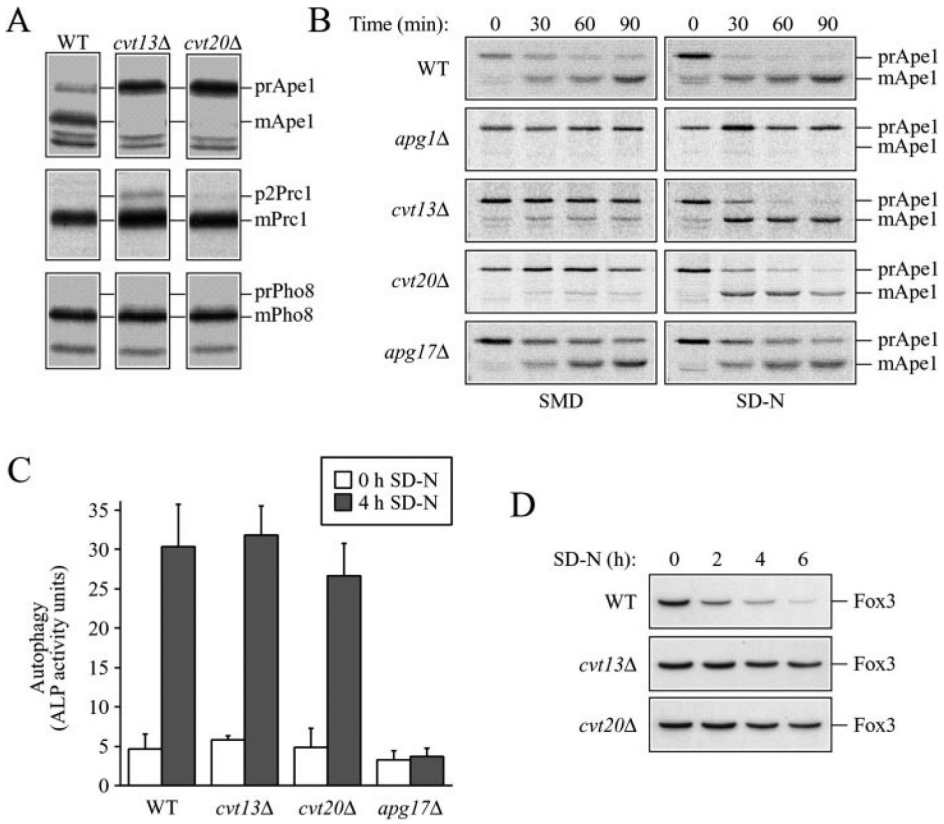

Fig. 1. The *cvt13* and *cvt20* mutants are specifically defective in the Cvt pathway

A, processing of vacuolar hydrolases. Cells from wild type (*WT*) (SEY6210), *cvt13*Δ, and *cvt20*Δ strains were pulse-labeled for 10 min and chased for either 90 (Ape1) or 30 min (Prc1 and Pho8). Ape1, Prc1, and Pho8 were immunoprecipitated from cell lysates and resolved by SDS-PAGE. Prc1 and Pho8 processing was essentially normal in both mutant strains. *B*, kinetics of transport by the Cvt pathway. Cells from wild type (SEY6210), *apg1*Δ (NNY20), *cvt13*Δ (D3Y108), *cvt20*Δ (D3Y109), and *apg17*Δ strains were pulse-labeled for 10 min in SMD, washed, and resuspended in either SMD or SD-N medium, and chased for the indicated times. Ape1 was immunoprecipitated from cell lysates and resolved by SDS-PAGE. Note that there is a background band that migrates just below the position of mApe1. *C*, Pho8 activity assay for autophagy. Wild type (TN124), *cvt13*Δ (D3Y111), *cvt20*Δ (D3Y112), and *apg17*Δ (D3Y113) cells expressing Pho8Δ60 were shifted from nutrient-rich medium (*white bars*) to SD-N medium (*black bars*) for 4 h. Autophagy induction was determined by a Pho8 activity assay as described under “Experimental Procedures.” *Error bars* represent the standard deviation from three separate experiments. The *cvt13* and *cvt20* mutants are not defective in autophagic induction. *D*, pexophagy analysis. Cells from wild type (BY4742) and the *cvt13*Δ and *cvt20*Δ mutant strains in the BY4742 background were grown under conditions that induce peroxisomes (see “Experimental Procedures”), washed, and resuspended in SD-N for the time indicated. The presence of the peroxisomal thiolase enzyme, Fox3, was detected by immunoblotting. The *S. cerevisiae* strains *cvt13*Δ and *cvt20*Δ are defective in pexophagy.

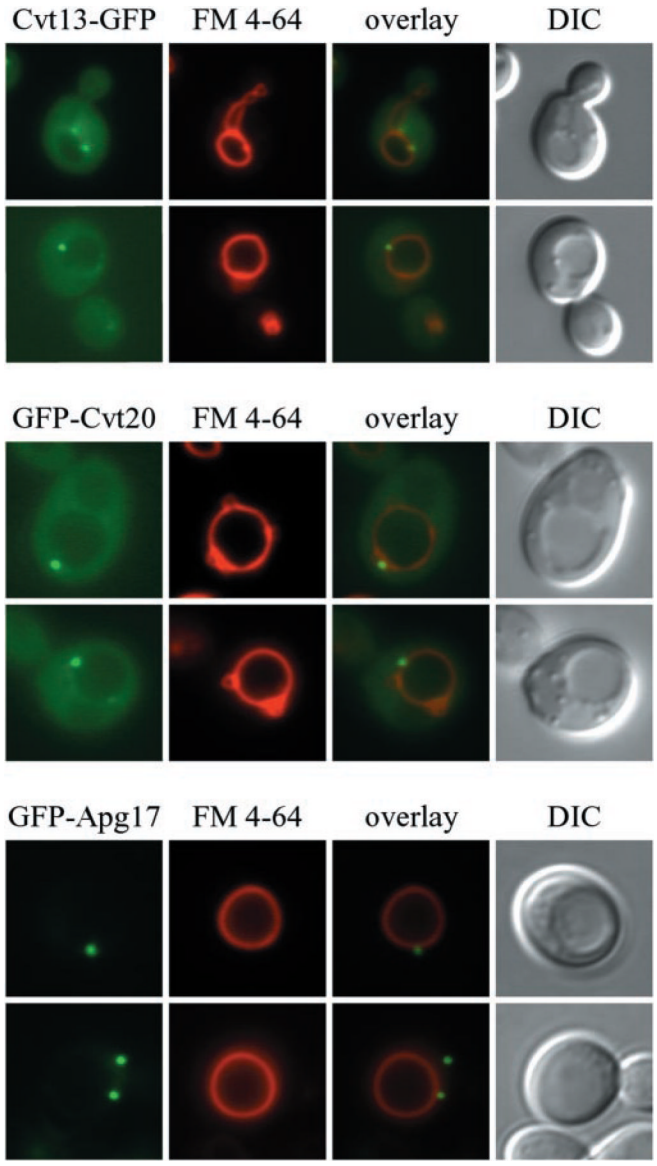

Fig. 2. Localization of Cvt13-GFP, GFP-Cvt20, and GFP-Apg17

The *cvt13*Δ (D3Y108), *cvt20*Δ (D3Y109), and *apg17*Δ strain were transformed with plasmids encoding GFP fused to the carboxyl or amino termini of the corresponding ORFs (pCVT13-GFP, pGFP-CVT20 and pGFP-APG17, respectively). Cells were grown in SMD, treated with FM 4-64 to label vacuoles, and visualized by fluorescence microscopy as described under "Experimental Procedures." Cvt13-GFP and GFP-Cvt20 display punctate perivacuolar dots and diffuse cytosolic staining. *DIC*, differential interference contrast.

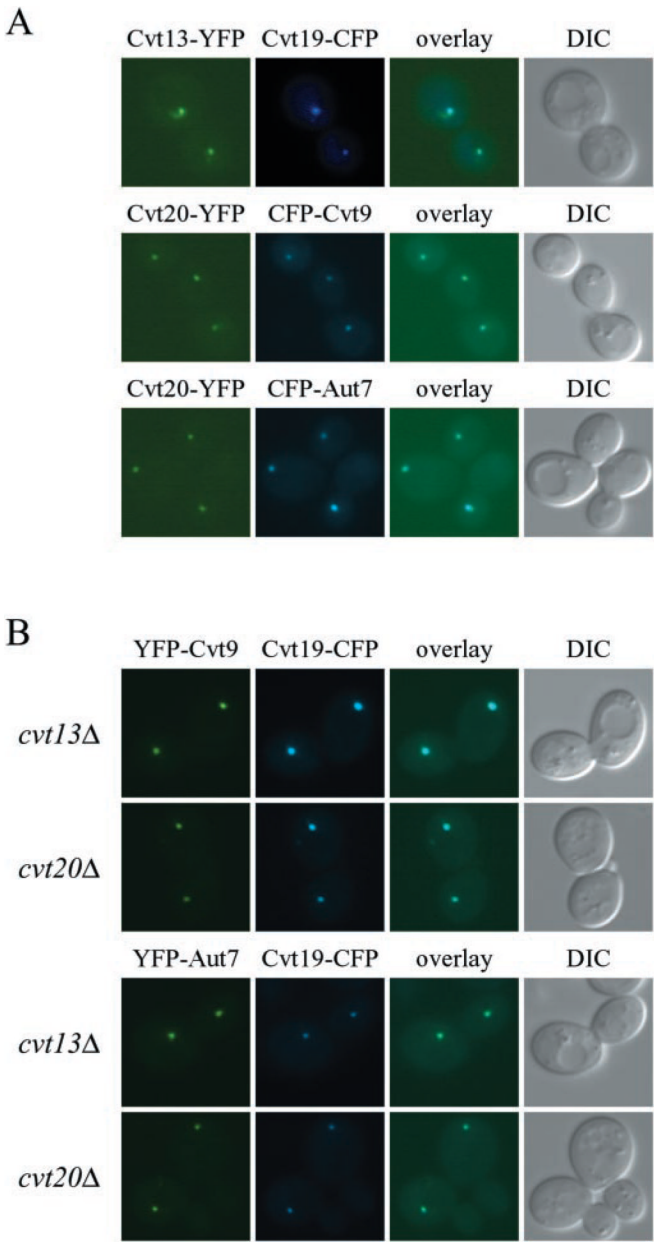

Fig. 3. Cvt13, Cvt20, Cvt9, the cargo specificity factor Cvt19, and the vesicle component Aut7 co-localize on a punctate, perivacuolar structure

A, cells of strains PSY14 (*CVT13-YFP*) and PSY15 (*CVT20-YFP*) were transformed with pCVT19-CFP, pCuCFP-CVT9, or pCuCFP-AUT7. Transformed cells were grown to midlog stage in SMD and shifted to YPD for 2–3 h prior to microscopy analysis. Images were captured and analyzed as described under "Experimental Procedures." *B*, co-localization of Cvt19 with Cvt9 and Aut7 occurs independent of Cvt13 and Cvt20. D3Y108 (*cvt13*Δ) and D3Y109 (*cvt20*Δ) cells expressing YFP-Cvt9 or YFP-Aut7 along with Cvt19-CFP were prepared and examined as in *A*. *DIC*, differential interference contrast.

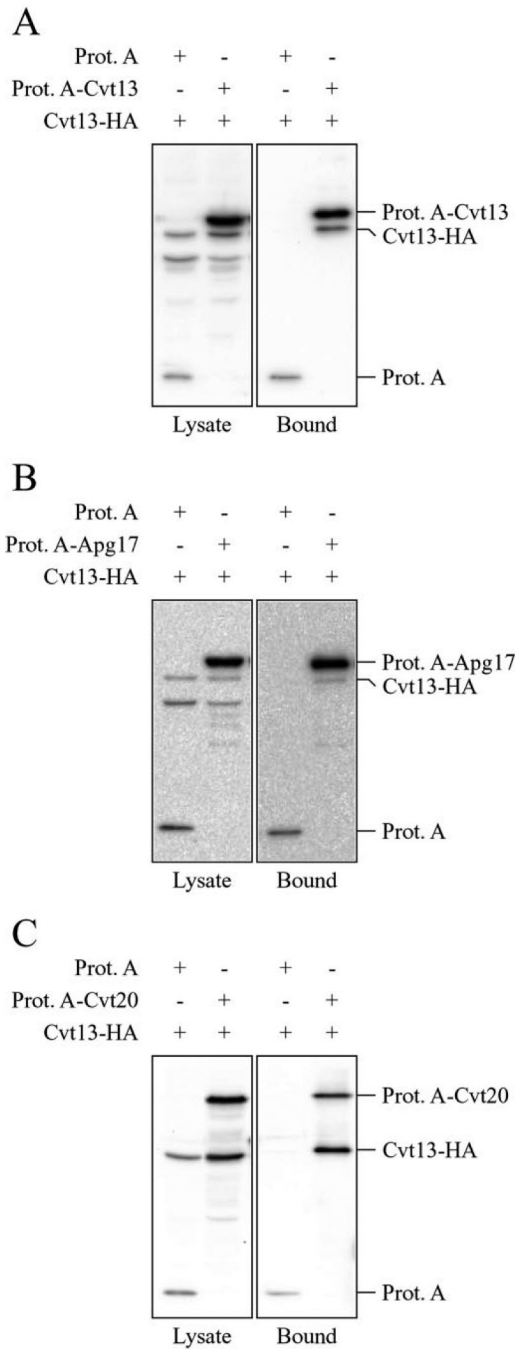

Fig. 4. Cvt13 associates with Cvt20 and Apg17

Detergent-solubilized extracts from wild type (SEY6210) cells expressing Cvt13-HA and protein A (*Prot. A*) and Cvt13-HA and either protein A-Cvt13 (*A*), protein A-Apg17 (*B*), or protein A-Cvt20 (*C*) were prepared as described under "Experimental Procedures." Associated proteins were isolated with IgG-coated Dynabeads and visualized by immunoblotting with antiserum to HA. For each experiment ~2% of the total lysate or 10% of the total eluate was loaded per lane.

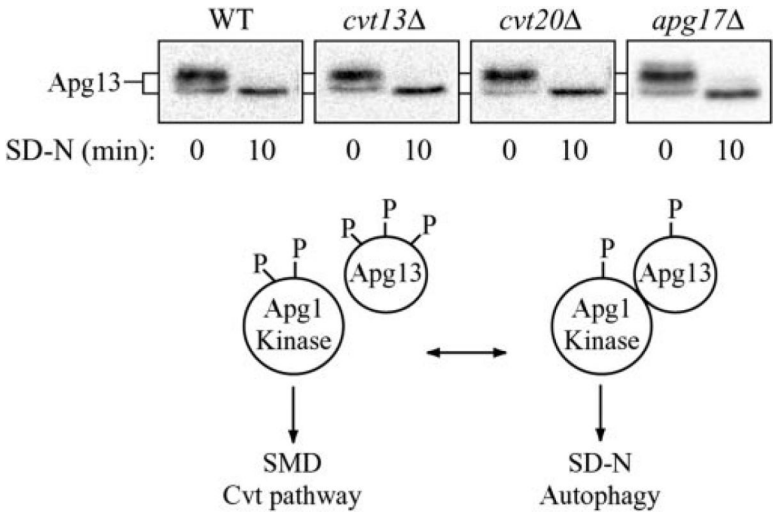

Fig. 5. Phosphorylation state of Apg13

Cells from wild type (*WT*) (SEY6210), *cvt13*Δ (D3Y108), *cvt20*Δ (D3Y109), or *apg17*Δ strains over-expressing Apg13 were grown in SMD and then shifted to SD-N at time 0. Samples were collected after 10 min, and Apg13 was detected by immunoblotting. Nutrient-dependent dephosphorylation of Apg13 is normal in strains *cvt13*Δ, *cvt20*Δ, and *apg17*Δ. A schematic representation of the Apg13 dephosphorylation and interaction with Apg1 is depicted *below* the blots.

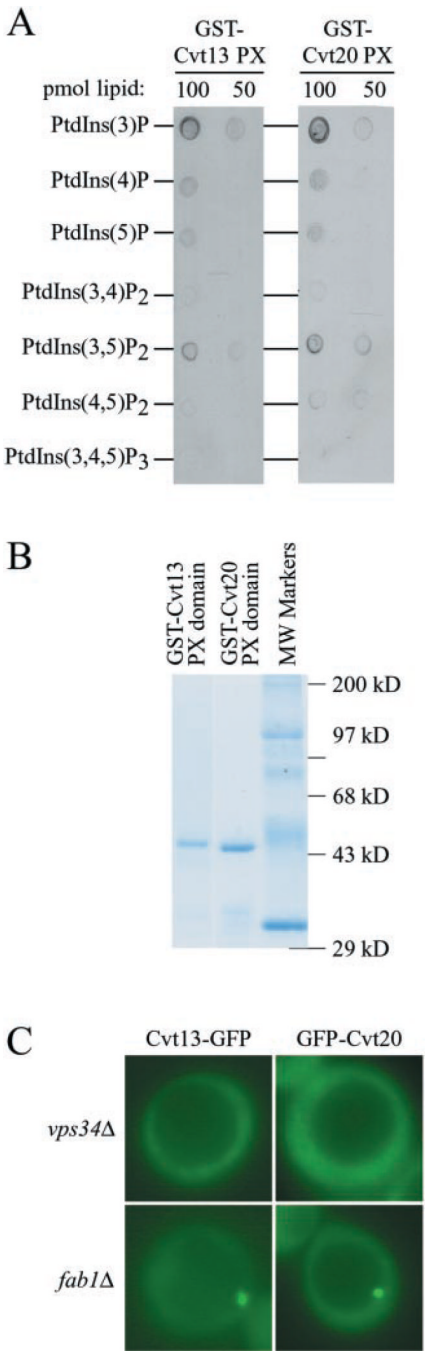

Fig. 6. Specific phosphatidylinositol 3-phosphate (*PtdIns(3)P*) recognition by the Cvt20 PX domain

A, protein-lipid overlay assay. Serial dilutions of phosphoinositides were spotted onto nitrocellulose membrane and incubated with purified GST-Cvt13 PX or GST-Cvt20 PX domain fusion protein. The membrane was washed and analyzed by immunoblot with antibodies to GST. *B*, Coomassie-stained gel of purified GST-Cvt13 PX and GST-Cvt20 PX domain fusion protein. *C*, PtdIns(3)P-dependent localization of Cvt13-GFP and GFP-Cvt20 by fluorescence microscopy. Cells from *vps34*Δ and *fab1*Δ strains expressing either Cvt13-GFP or GFP-Cvt20 were grown in SMD and visualized by fluorescence microscopy.

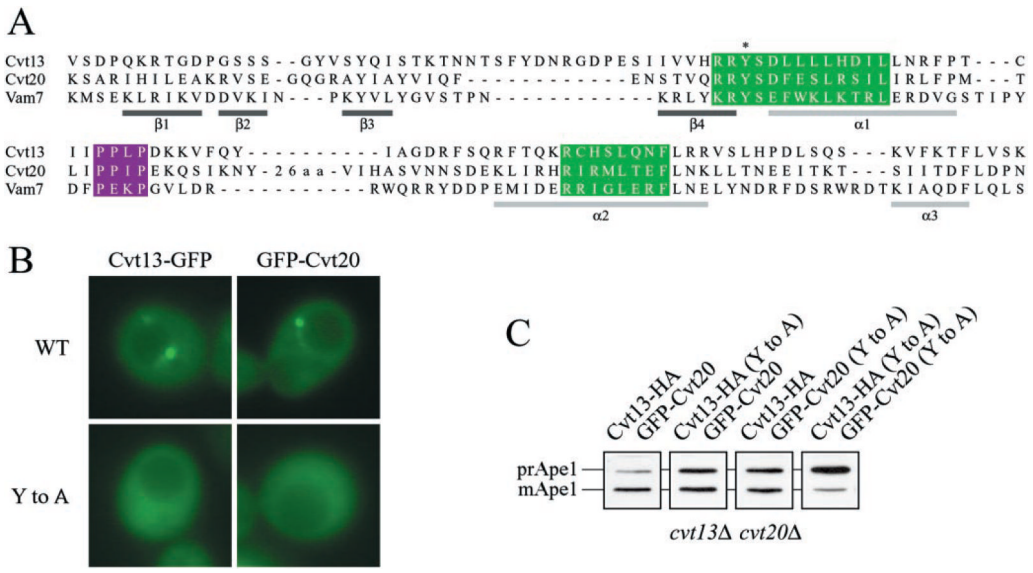

Fig. 7. Mutations in the PX domain of Cvt13 and Cvt20 abolish punctate localization and prApe1 trafficking

A, alignment of PX domain sequences (17,24). Elements of Vam7 secondary structure are shown *below* the sequences (24). Two highly conserved PX domain sequence motifs, (R/K)(R/K)(Y/F)*XX*F*XX*L*XXX*L and R(R/K)*XX*L*XX*(Y/F), are highlighted in *green* and the proline-rich motif, P*XX*P, is highlighted in *purple* (reviewed in Ref. 15). The Cvt13 and Cvt20 point mutations are indicated by an *asterisk*. *B*, Cvt13 and Cvt20 punctate localization requires a functional PX domain. D3Y108 (*cvt13*Δ) cells expressing Cvt13-GFP (*WT*) or Cvt13^{Y79A}-GFP (Tyr to Ala (Y to A)) and D3Y109 (*cvt20*Δ) cells expressing GFP-Cvt20 (*WT*) or GFP-Cvt20^{Y193A} (Tyr to Ala (Y to A)) were grown in SMD and visualized by fluorescence microscopy. *C*, prApe1 trafficking requires functional Cvt13 and Cvt20 PX domains. PSY10 (*cvt13*Δ *cvt20*Δ) cells expressing combinations of Cvt13-HA, GFP-Cvt20, Cvt13^{Y79A}-HA, and GFP-Cvt20^{Y193A}, as indicated, were grown to midlog phase in SMD. Protein extracts were prepared and analyzed by immunoblot with antiserum to Ape1.

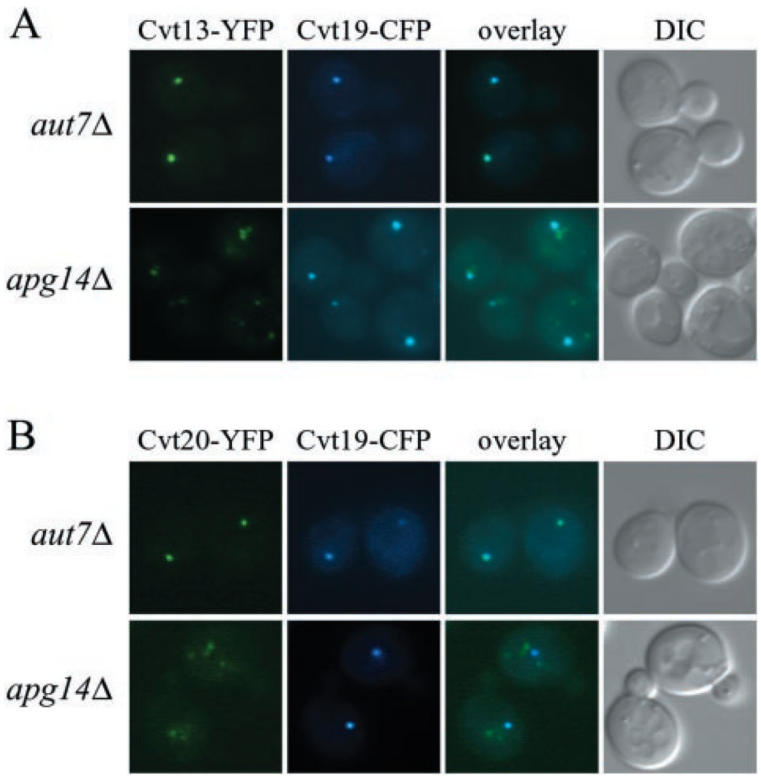

Fig. 8. Deletion of *APG14* disrupts Cvt13 and Cvt20 co-localization with Cvt19

The *aut7*Δ and *apg14*Δ strains expressing chromosomal Cvt13-YFP or Cvt20-YFP, PSY24, PSY25, PSY26 and PSY27, respectively, were transformed with pCVT19-CFP. Cells were prepared and examined as in Fig. 3. Contrast was enhanced for YFP in the *apg14*Δ strain relative to the *aut7*Δ strain to allow detection of the Cvt13-YFP and Cvt20-YFP signals. *DIC*, differential interference contrast.

Table I

S. cerevisiae strains used in this study

Strain	Genotype	Ref.
SEY6210	*MATα leu2–3,112 ura3–52 his3-Δ200 trp1-Δ901 lys2–801 suc2-Δ9 GAL*	45
TN124	*MATa leu2–3,112 trp1 ura3–52 pho8::pho8Δ60 pho13Δ::LEU2*	35
BY4742	*MATα his3Δ leu2Δ lys2Δ ura3Δ*	ResGen
cvtl3Δ	BY4742 *cvt13Δ::KAN*	ResGen
cvt20Δ	BY4742 *cvt20Δ::KAN*	ResGen
apg17Δ	BY4742 *apg17Δ::KAN*	ResGen
apg9Δ	BY4742 *apg9Δ::KAN*	ResGen
fab1Δ	BY4742 *fab1Δ::KAN*	ResGen
vps34Δ	SEY6210 *vps34Δ::TRP1*	41
NNY20	*MATa leu2–3,112 trp1 ura3–52 apg1Δ::LEU2*	7
D3Y108	SEY6210 *cvt13Δ::HIS3 S.k.*	This study
D3Y109	SEY6210 *cvt20Δ::HIS3 S.k.*	This study
D3Y111	TN124 *cvt13Δ::TRP1*	This study
D3Y112	TN124 *cvt20Δ::TRP1*	This study
D3Y113	TN124 *apg17Δ::TRP1*	This study
PSY10	D3Y108 *cvt20Δ::TRP1*	This study
PSY13	D3Y112 *cvt13Δ::KAN*	This study
PSY14	SEY6210 *cvt13-YFP::HIS5 S.p.*	This study
PSY15	SEY6210 *cvt20-YFP::HIS5 S.p.*	This study
WPHYD7	SEY6210 *aut7Δ::LEU2*	25
PSY24	WPHYD7 *cvt13-YFP::HIS5 S.p.*	This study
PSY25	WPHYD7 *cvt20-YFP::HIS5 S.p.*	This study
KTY1003	SEY6210 *apg14Δ::LEU2*	This study
PSY26	KTY1003 *cvt13-YFP::HIS5 S.p.*	This study
PSY27	KTY1003 *cvt20-YFP::HIS5 S.p.*	This study